

# Phospholipid Monolayer Density Distribution Perpendicular to the Water Surface. A Synchrotron X-Ray Reflectivity Study

To cite this article: C. A. Helm *et al* 1987 *EPL* **4** 697

View the [article online](#) for updates and enhancements.

## You may also like

- [EVOLUTION OF SYNCHROTRON X-RAYS IN SUPERNOVA REMNANTS](#)  
Ryoko Nakamura, Aya Bamba, Tadayasu Dotani *et al.*
- [Probing the Electrode-Electrolyte Interface in Cycled  \$\text{LiNi}\_{0.5}\text{Mn}\_{1.5}\text{O}\_4\$  by XPS Using Mg and Synchrotron X-rays](#)  
Azzam N. Mansour, David G. Kwabi, Ronald A. Quinlan *et al.*
- [Analysis of the induction of the myelin basic protein binding to the plasma membrane phospholipid monolayer](#)  
Lei Zhang, , Changchun Hao *et al.*

## Phospholipid Monolayer Density Distribution Perpendicular to the Water Surface. A Synchrotron X-Ray Reflectivity Study.

C. A. HELM(\*), H. MÖHWALD(\*), K. KJÆR(\*\*) and J. ALS-NIELSEN(\*\*)

(\*) *T.U. Munich, Physics Dept. E22 (Biophysics) - D-8046 Garching, BRD*

(\*\*) *Physics Department, Risø National Laboratory - DK-4000 Roskilde, Denmark*

(received 18 March 1987; accepted 11 June 1987)

PACS. 61.10. – X-ray determination of structures.

PACS. 87.20. – Membrane biophysics.

PACS. 68.10. – Fluid surfaces and interfaces with fluids.

**Abstract.** – Phospholipid monolayers at the air-water interface have been studied by synchrotron X-ray reflection methods. The range of momentum transfers (perpendicular to the surface) exceeded  $2\pi/(\text{layer thickness})$  thus yielding information about the density distribution across the layer. Data for a monolayer of L- $\alpha$ -dipalmitoylphosphatidylcholine (DPPC) in the solid phase (surface pressure 40 mN/m) are interpreted in terms of a simple model of the density with adjustable values for the densities and the projected lengths of the aliphatic tail and the polar head as well as an overall Gaussian smearing of the densities. We find that the tails are close-packed but uniformly tilted  $30^\circ$  relative to the interface normal.

### 1. Introduction.

Lipid monolayers at the air/water interface have been shown to be good models for studying processes involving biological membranes [1, 2] but also for the study of the physics of two-dimensional systems [3]. Furthermore, information on the structure of surfactants on water is relevant for the applications of Langmuir-Blodgett films which are transferred from the water surface to a solid support. These films have many potential technical applications [4].

However, information about the microscopic structure has traditionally been inferred from macroscopic thermodynamic data, partly supplemented by surface potential measurements [5, 6]. Considerable progress has recently been achieved by developments of optical microscopy [7] and spectroscopy [8] using dye molecules in dilute concentrations. The spatial resolution of these techniques is in the micron range and there is thus an urgent need to develop techniques with nanometer resolution—the molecular-size range. Obvious possibilities are X-ray diffraction or reflection studies. These techniques are now feasible by utilizing the brightness of synchrotron X-ray sources [9]. Previous reflectivity studies include the roughness of the water surface [10] and smectic layering at the surface of liquid crystal materials [11, 12]. As an extension of this work we have recently observed, for the

first time, diffraction peaks from the in-plane structure of a phospholipid monolayer prepared in a Langmuir film balance placed *in situ* at the sample stage of the diffractometer [13-15]. This study revealed a decoupling between the bond orientational and positional ordering in the so-called gel phase. Using the same set-up we, report in this work on the out-of-plane structure by X-ray reflectivity measurements. The sample was a monolayer of the phospholipid L- $\alpha$ -dipalmitoylphosphatidylcholine, DPPC, in the solid phase at two temperatures, 10 °C and 23 °C. The data are interpreted in terms of a simple model of the projection of the electron density onto the surface normal.

## 2. Experimental.

The phospholipid monolayer was prepared in a Langmuir trough enclosed in a gas tight canister by spreading a chloroform/methanol solution of the water surface and monitoring the surface pressure by a Wilhelmy film balance. The phospholipid was used as delivered (Sigma, Munich) without any further purification. The water was millipore filtered. The diffractometer set-up at beamline D4 at HASYLAB, DESY, Hamburg, has been described previously [15]. In short, the reflectivity is measured *vs.* glancing angle  $\alpha$  at a wavelength of 1.38 Å or wave vector  $k = 4.55 \text{ \AA}^{-1}$ . The angular resolution and reproducibility is around 0.005°. We present the reflectivity as a function of the normalized wave vector transfer  $Q/Q_c$ , where  $Q \equiv 2k \sin(\alpha)$  and  $Q_c = 2k \sin(\alpha_c) = 0.0217 \text{ \AA}^{-1}$ .  $\alpha_c$  is the critical angle for total reflection from water. The reflectivity  $R$  is given as  $R/R_{\text{Fres.}}$ , where  $R_{\text{Fres.}}$  is the «Fresnel» reflectivity calculated (without any adjustable parameters) for a discontinuous jump in the electron density from air to water (ref. [16]). For  $Q \gg Q_c$ ,  $R_{\text{Fres.}}$  falls off as  $(Q_c/2Q)^4$ . Data presented in this form are given in fig. 1a), 3a) and 4a). The minimum observed near

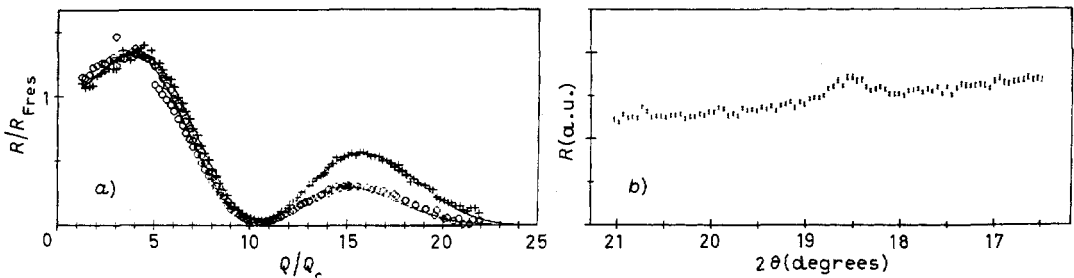


Fig. 1. - a) Normalized X-ray reflectivity as a function of the normalized perpendicular wave vector transfer for a DPPC monolayer at 10 °C (crosses) and at 23 °C (circles). Two data sets were taken at the latter temperature on the same film but at different times. There is some discrepancy in the region around  $Q/Q_c = 5 \div 8$  which, however, does not alter the best-fit model parameters significantly. b) Diffracted intensity as a function of horizontal diffraction angle  $2\theta$  for the DPPC monolayer of fig. 1a), at 23 °C. Background not subtracted.

$Q = 10.5 * Q_c$  results from destructive interference and allows the determination of the phospholipid layer thickness. The surface pressure was maintained above 40 mN/m, which is well above the pressure of 15 mN/m, where the transition to the «solid» phase occurs [6]. In this phase, the molecular area is  $46 \text{ \AA}^2$  ( $23 \text{ \AA}^2$  per hydrocarbon chain). At this pressure, one can observe a diffraction peak, albeit weak, at a horizontal scattering angle  $2\theta$  around 18.5°, see fig. 1b). Our previous studies [13-15] (dimyristoylphosphatidic acid) demonstrated a more intense diffraction peak which may be due to a more favourable value of the structure factor.

### 3. Interpretation.

The reflectivity  $R(Q)$  relative to the Fresnel reflectivity  $R_{\text{Fres.}}(Q)$  is related to the density gradient  $d\rho/dz$  by [16]

$$R(Q)/R_{\text{Fres.}}(Q) = \left| \int (d\rho/dz) \exp[iQz] dz \right|^2, \quad (1)$$

$\rho$  is the electron density normalized to the electron density in bulk water. Using eq. (1) we shall now interpret the data, more conveniently displayed on a logarithmic reflectivity scale in fig. 3 and 4, in terms of a density model.

The density model is sketched in fig. 2. To begin with, we assume two constant-density regions of the molecule: a hydrocarbon tail region and a polar head region. However, this density box model is smeared, partly due to the diffuseness of the atomic electron clouds,

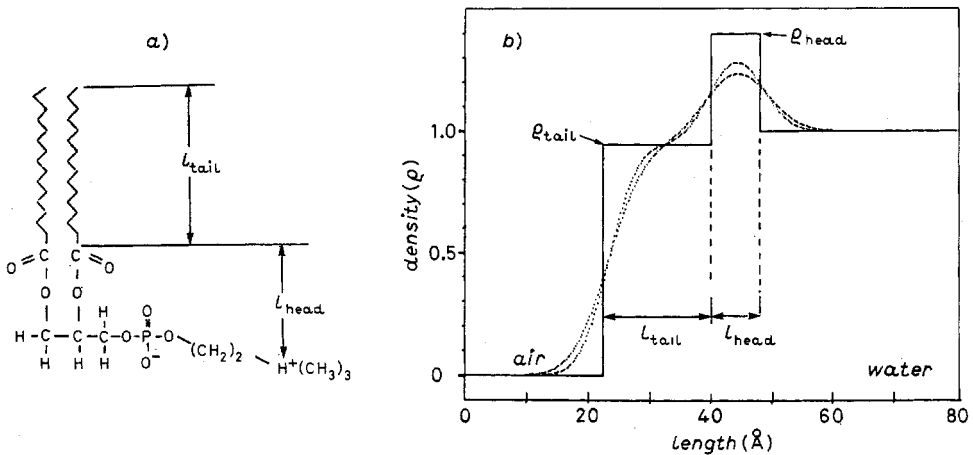


Fig. 2. – Molecular structure (a) and model of the density (b). The full line in b) shows the box model (prior to smearing) with the parameters fitted for the data at 23 °C (see text). The dotted curves show the actual smeared density models fitted to the data. The larger smearing corresponds to the higher temperature.

partly due to thermal roughness, cf. ref. [10]. The model then contains 5 adjustable parameters: 2 box heights (densities), 2 box widths (lengths of projected molecular segments) and an overall smearing parameter. An example of the box model is shown in fig. 2a), using parameters that are shown below to fit the data. The dotted lines show the Gaussian smearing of the box model according to  $\exp[-z^2/2\sigma^2]$ . The two curves correspond to data at 23 °C and 10 °C.

Before comparing the model with the data, let us discuss physically reasonable values of the parameters. First the aliphatic tail. The maximal extension  $l^{\text{max}}$  of an aliphatic chain of  $n$ -CH<sub>2</sub> groups in all-*trans* configurations amounts to [17, 18]

$$l^{\text{max}} = 1.5 + n * 1.265 \text{ \AA}, \quad (2)$$

$$= 19.2 \text{ \AA} \quad \text{for DPPC}.$$

The maximal density of electrons (relative to the electron density in bulk water) is

$$\rho^{\max} = 0.945, \quad (3)$$

corresponding to a volume of  $25.3 \text{ \AA}^3$  per  $\text{CH}_2$  group is close-packing. This agrees within one per cent with either of ref. [19, 20]. The area per  $\text{CH}_2$  chain in close-packed configuration is about  $20 \text{ \AA}^2$  (ref. [20]). For DPPC monolayers the area per chain according to the isotherms is  $23 \text{ \AA}^2$  [6]. The density corresponding to all-*trans* configuration chains perpendicular to the surface is thus  $(20/23) * 0.945 = 0.822$ , which may be taken as a lower limit of physically reasonable values of  $\rho_{\text{tail}}$ .

Next we discuss the polar head group. The choline part has nearly the same density as water and thus cannot be distinguished from water in the reflectivity measurements. The phosphate part can assume different configurations. Judged from space-filling molecular models the dimension perpendicular to the surface is within the limits of

$$5 \text{ \AA} < l_{\text{head}} < 9 \text{ \AA}. \quad (4)$$

For the maximum extension of the phosphate group perpendicular to the water surface ( $9 \text{ \AA}$ ), and using the thermodynamic value of  $46 \text{ \AA}^2$  for the area per molecule, we estimate a minimal normalized density of the head group region of about 1.3. This includes a contribution from water (or the choline group) penetrating into the space available between the phosphates. A maximal head group density of 1.7 results from assuming the minimal extension of  $5 \text{ \AA}$ , and an area per chain of  $20 \text{ \AA}^2$ .

We shall now consider a best fit of the model to the data. In fig. 3 we have assumed close packing of the electron density in the tails, *i.e.*  $\rho_{\text{tail}} = 0.945$ . Trial values for the head density

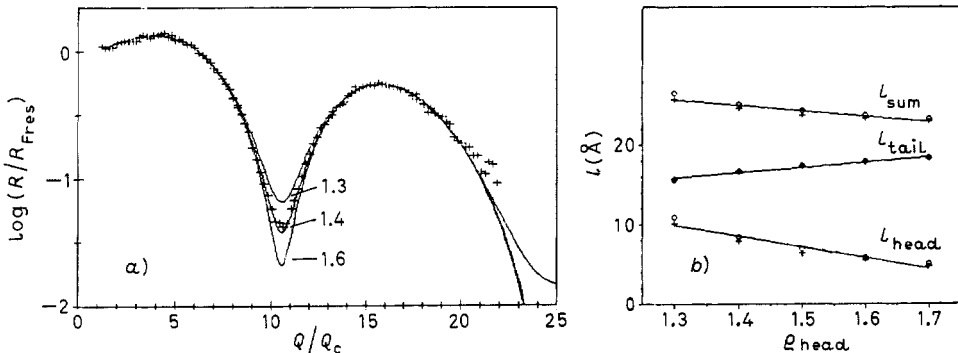


Fig. 3. - a) Best fits of the reflectivity data (at  $10^\circ\text{C}$ ) for  $\rho_{\text{tail}} \equiv 0.945$  and varying  $\rho_{\text{head}}$  as indicated. b)  $l_{\text{sum}}$ ,  $l_{\text{tail}}$  and  $l_{\text{head}}$  obtained from the fits for  $\rho_{\text{tail}} \equiv 0.945$  and various  $\rho_{\text{head}}$  for temperatures of  $10^\circ\text{C}$  (crosses) and  $23^\circ\text{C}$  (circles).

are 1.3, 1.4, 1.5, 1.6 and 1.7, respectively. For fixed densities the lengths of the head and tail and the smearing have been least-squares fitted. The resulting values of  $l_{\text{tail}}$  and  $l_{\text{head}}$  vs.  $\rho_{\text{head}}$  are shown in fig. 3b). Figure 3a) shows that parameter values of  $\rho_{\text{tail}} = 0.945$ ,  $\rho_{\text{head}} = 1.4$ ,  $l_{\text{head}} = 7.9 \text{ \AA}$ ,  $l_{\text{tail}} = 16.7 \text{ \AA}$  and  $\sigma = 3.7 \text{ \AA}$  fit the data at  $10^\circ\text{C}$  very well. It also shows that the sensitivity to the value of  $\rho_{\text{head}}$  is better than 5%. The sensitivity to values of  $\rho_{\text{tail}}$  is even higher. This is illustrated in fig. 4 which is analogous to fig. 3 but with  $\rho_{\text{head}}$  kept fixed at 1.4 and  $\rho_{\text{tail}}$  as parameter. (We have also tried other combinations of  $\rho_{\text{head}}$  and  $\rho_{\text{tail}}$

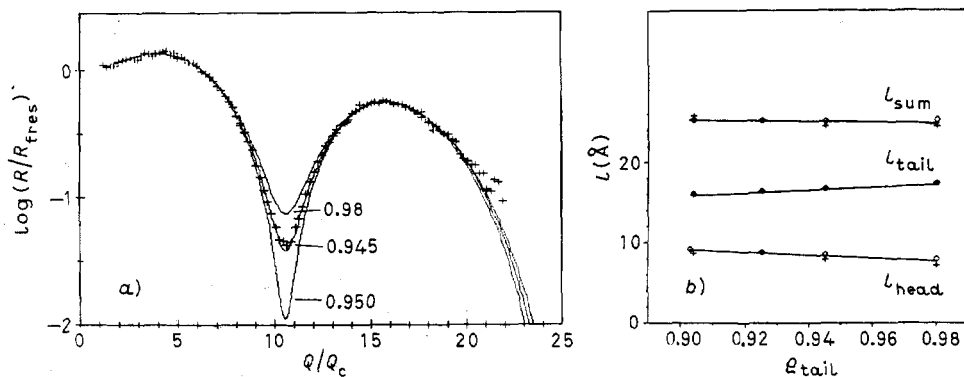


Fig. 4. - a) Best fits of the reflectivity data (at  $10^\circ\text{C}$ ) for  $\rho_{\text{head}} \equiv 1.40$  and varying  $\rho_{\text{tail}}$  as indicated. b)  $l_{\text{sum}}$ ,  $l_{\text{tail}}$  and  $l_{\text{head}}$  obtained from the fits for  $\rho_{\text{head}} \equiv 1.40$  and various  $\rho_{\text{tail}}$  for temperatures of  $10^\circ\text{C}$  (crosses) and  $23^\circ\text{C}$  (circles).

than those presented in fig. 3 and 4. These, however, all gave poorer agreement with the data or were insensible.) Figures 3b) and 4b) show that the length parameters are essentially independent of the temperature. Most important, the best value of  $l_{\text{tail}}$  is rather insensitive to the choice of densities and is definitely below the all-*trans*, straight-up value of  $19.2 \text{\AA}$ . This together with the best-fit value of  $\rho_{\text{tail}}$  coinciding precisely with the close-packed value for  $\text{CH}_2$  chains shows unambiguously that the chains are tilted and we can immediately infer the tilt angle  $\beta$  from

$$\cos(\beta) = l_{\text{tail}}/19.2 \text{\AA} \quad \text{or} \quad \beta = 30^\circ. \quad (5)$$

The phosphate-group dimension perpendicular to the water surface is about  $7.9 \text{\AA}$  at  $10^\circ\text{C}$  and  $8.4 \text{\AA}$  at  $23^\circ\text{C}$ . The r.m.s. smearing of tail and head group densities depends on the temperature,  $\sigma = 3.7 \text{\AA}$  at  $10^\circ\text{C}$  and  $\sigma = 4.4 \text{\AA}$  at  $23^\circ\text{C}$ . These values are somewhat larger than the thermal roughness of water,  $\sigma = 3.2 \text{\AA}$  (ref. [10]), presumably due to the reduced surface tension of the film compared to water. The other parameters,  $l_{\text{tail}}$ ,  $\rho_{\text{tail}}$ , and  $\rho_{\text{head}}$  have the same values at  $10^\circ\text{C}$  and at  $23^\circ\text{C}$ .

#### 4. Discussion and conclusions.

The reflectivity data span wave vector transfers up to twice the characteristic value of  $2\pi/(\text{film thickness})$  and deviations of more than an order of magnitude from the Fresnel law are observed. It is, therefore, not surprising that data of this type contain detailed information about the density profile across the film, as discussed above.

We have found that the parameters deduced from the reflectivity data imply that the tails are close-packed but uniformly tilted  $30^\circ$  from the surface normal. Tilted chains were inferred as well from polarization studies with fluorescent dye molecules in DPPC monolayers [21] and from X-ray studies of DPPC vesicles [22]. The area per close-packed chain is  $20 \text{\AA}^2$  at  $\beta = 0$  and increases with tilt angle  $\beta$  as  $1/\cos(\beta)$ . A tilt angle of  $30^\circ$  then implies an area of  $23 \text{\AA}^2$  per chain or  $46 \text{\AA}^2$  per molecule in agreement with the thermodynamic data. A uniform tilt of the chains will imply a distortion of the hexagonal in-plane lattice and accordingly a splitting of the (1, 0) diffraction peak into at least 2 peaks. We have not been able to detect this splitting, but the structure factors are not known and the

diffracted intensities are at any rate very weak. It should be noted though, that the shortest reciprocal lattice vector in the distorted lattice will be along the projected tilt direction with a structure factor reflecting the density modulation of the projected chains. At a tilt angle of  $30^\circ$ , the projected density from neighbouring chains will overlap, thus reducing the density modulation and diminishing the corresponding structure factor. Electron diffraction data from a Langmuir-Blodgett film of DPPC [23] either had insufficient resolution to observe this splitting or else this subtle effect of the structure was lost in drawing the film onto a solid substrate. The diffraction pattern in fig. 1b) consisting of a single, weak peak at a scattering angle of  $18.5^\circ$  (corresponding to a  $d$ -spacing of  $4.28 \text{ \AA}$ ) is thus not inconsistent with a uniform tilt of the chains or a molecular area of  $46 \text{ \AA}^2$ .

Concerning the model parameters in the head group region, as discussed above they are consistent with molecular dimensions, but the detailed arrangement of the atoms in the head group cannot be inferred by this method. Our data are in accordance with measurements of the partial molecular volume,  $v$ , in lipid vesicles. For DPPC one finds [24]  $v = 1130 \text{ \AA}^3$  at  $20^\circ\text{C}$ . From our data one can calculate  $v = \text{\AA}^2 * l_{\text{sum}} = 1160 \text{ \AA}^3$ . This includes the contribution of water molecules penetrating in amongst the loosely packed head groups.

Since DPPC is not charged, the model here presented does not include the effect of a Gouy-Chapman charge distribution below a charged monolayer. However, we have observed a distinct change in the reflectivity profile  $R(Q)$  with ionic strength for monolayers of the charged phospholipid DMPA. Analysis of this kind of data will be the subject of a subsequent paper.

Reflectivity data from a film of amphiphilic  $\alpha$ -aminoacid used as precursor for epitaxial growth of aminoacid crystals have been analysed by the methods presented in this work [25].

\* \* \*

We thank J. ENGELHARDT for providing us with parts of the fitting programs used in the analysis. This work was supported by the German Bundesministerium for Research and Technology (BMFT) and by the Danish National Science Foundation (SNF).

## REFERENCES

- [1] PHILLIPS M. C. and CHAPMAN D., *Biochim. Biophys. Acta*, **163** (1968) 301.
- [2] VERGER R., PATTUS F., PIERONI G., RIVIERE C., FERRATO F., LEONARDI J. and DARGENT B., *Colloid Surf.*, **10** (1984) 163.
- [3] NELSON D. R., RUBINSTEIN M. and SPAEPEN F., *Philos. Mag.*, **46** (1982) 105.
- [4] ROBERTS G. G., *Adv. Phys.*, **34** (1985) 475.
- [5] GAINES G. L. jr., *Insoluble Monolayers at Liquid-Gas Interfaces* (Interscience, New York, N. Y.) 1966.
- [6] ALBRECHT O., GRULER H. and SACKMANN E., *J. Phys. (Paris)*, **39** (1978) 301.
- [7] LÖSCHE M., SACKMANN E. and MÖHWALD H., *Ber. Bunsenges. Phys. Chem.*, **87** (1983) 848.
- [8] MÖBIUS D., ORRIT M., GRÜNINGER H. and MEYER H., *Thin Solid Films*, **132** (1985) 41.
- [9] SEUL M., EISENBERGER P. and MCCONNELL H. M., *Proc. Natl. Acad. Sci. USA*, **80** (1983) 5795.
- [10] BRASLAU A., DEUTSCH M., PERSHAN P. S., WEISS A. H., ALS-NIELSEN J. and BOHR J., *Phys. Rev. Lett.*, **54** (1985) 114.
- [11] ALS-NIELSEN J. and PERSHAN P. S., *Nucl. Instrum. Methods*, **208** (1983) 545.
- [12] ALS-NIELSEN J., CHRISTENSEN F. and PERSHAN P. S., *Phys. Rev. Lett.*, **48** (1982) 1107.
- [13] MÖHWALD H., in *The Physics and Fabrication of Microstructures and Microdevices*, edited by M. J. KELLY and C. WEISBUCH, *Springer Series in Physics*, **13** (1986) 186.

- [14] KJÆR K., ALS-NIELSEN J., HELM C. A., LAXHUBER L. T. and MÖHWALD H., *Phys. Rev. Lett.*, **58** (1987) 2224.
- [15] HELM C. A., MÖHWALD H., KJÆR K. and ALS-NIELSEN J., to appear in *Biophys. J.* (1987).
- [16] ALS-NIELSEN J., in *Structure and Dynamics of Surfaces*, Vol. 2, ch. 5 edited by W. SCHOMMERS and P. BLANCKENHAGEN, *Topics in Current Physics* (Springer, Berlin) 1986.
- [17] TANFORD C., *The Hydrophobic Effect* (Wiley, New York, N.Y.) 1973.
- [18] ISRAELACHVILI J. N., *Intermolecular and Surface Forces*, ch. 16.3. (Academic Press, New York, N.Y.) 1985.
- [19] TARDIEU A., LUZZATI V. and REMAN F. C., *J. Mol. Biol.*, **75** (1973) 711.
- [20] NAGLE J. F. and WILKINSON D. A., *Biophys J.*, **23** (1978) 159.
- [21] MOY V. T., KELLER D., GAUB H. E. and MCCONNELL H. M., *J. Phys. Chem.*, **90** (1986) 3198.
- [22] JANIÁK M. J., SMALL D. M. and SHIPLEY G. G., *Biochemistry*, **15** (1976) 4575.
- [23] FISCHER A. and SACKMANN E., *J. Phys. (Paris)*, **45** (1984) 517.
- [24] SCHMIDT G. and KNOLL W., *Ber. Bunsenges. Phys. Chem.*, **89** (1985) 36.
- [25] WOLF S. G., LEISEROWITZ L., LAHAV M., DEUTSCH M., KJÆR K. and ALS-NIELSEN J., to appear in *Nature* (1987).